Hindawi
International Transactions on Electrical Energy Systems
Volume 2023, Article ID 9787820, 1 page
https://doi.org/10.1155/2023/9787820

Retraction

Retracted: Improved VMD-+ACO Algorithm Navigation and Positioning Technology for Robot Electric Power Inspection

International Transactions on Electrical Energy Systems

Received 19 September 2023; Accepted 19 September 2023; Published 20 September 2023

This article has been retracted by Hindawi following an investigation undertaken by the publisher [1]. This investigation has uncovered evidence of one or more of the following indicators of systematic manipulation of the publication process:

(1) Discrepancies in scope

(2) Discrepancies in the description of the research reported

(3) Discrepancies between the availability of data and the research described

(4) Inappropriate citations

(5) Incoherent, meaningless and/or irrelevant content included in the article

(6) Peer-review manipulation

The presence of these indicators undermines our confidence in the integrity of the article's content and we cannot, therefore, vouch for its reliability. Please note that this notice is intended solely to alert readers that the content of this article is unreliable. We have not investigated whether authors were aware of or involved in the systematic manipulation of the publication process.

Wiley and Hindawi regrets that the usual quality checks did not identify these issues before publication and have since put additional measures in place to safeguard research integrity.

We wish to credit our own Research Integrity and Research Publishing teams and anonymous and named external researchers and research integrity experts for contributing to this investigation.

The corresponding author, as the representative of all authors, has been given the opportunity to register their agreement or disagreement to this retraction. We have kept a record of any response received.

References

[1] Y. Long, M. Du, X. Luo, S. Li, and X. Jiang, "Improved VMD-+ACO Algorithm Navigation and Positioning Technology for Robot Electric Power Inspection," *International Transactions on Electrical Energy Systems*, vol. 2022, Article ID 5467622, 6 pages, 2022.

Hindawi
International Transactions on Electrical Energy Systems
Volume 2022, Article ID 5467622, 6 pages
https://doi.org/10.1155/2022/5467622

Research Article

Improved VMD-+ACO Algorithm Navigation and Positioning Technology for Robot Electric Power Inspection

Yingkai Long,[1] **Mingming Du**,[2] **Xiaoxiao Luo**,[1] **Siquan Li**,[1] **and Xiping Jiang**[1]

[1]*State Grid Chongqing Electric Power Research Institute, Chongqing 401121, China*
[2]*State Grid Chongqing Electric Power Company, Chongqing 400013, China*

Correspondence should be addressed to Yingkai Long; 201804202@stu.ncwu.edu.cn

Received 8 July 2022; Revised 17 August 2022; Accepted 24 August 2022; Published 12 September 2022

Academic Editor: Nagamalai Vasimalai

In order to meet the navigation and positioning requirements of force inspection robot, a new technology based on improved VMD- + ACO algorithm is proposed. The main content of this technology is based on the research of improved VMD algorithm and ACO algorithm, through the comparison of VMD algorithm and improved VMD algorithm. By using ACO parameter optimization design and so on, the research means of improving VMD- + ACO algorithm navigation and positioning technology of electric inspection robot is finally established through experiments and analysis. The experiment result shows the following. The minimum iteration number of the improved ACO is 112, which is 24.32% less than that of the basic ACO. The mean value of the worst value and the optimal value of the function are equal to 0. It shows that the improved ACO has higher convergence precision and the number of iterations is significantly reduced. *Conclusion*. Based on the improved VMD- + ACO algorithm, it can meet the navigation and positioning requirements of electric inspection robot.

1. Introduction

Power inspection robot is a regular or random inspection in the production and operation of products, aiming to find quality problems or operation faults of equipment in time [1]. At present, the traditional navigation solutions of inspection robot at home and abroad have certain limitations. Magnetic track and RFID tag schemes need to be embedded, which causes great damage to the ground and has high maintenance costs. GNSS schemes are easy to lose satellite signals in scenes with lots of occlusion and cannot be used indoors. The navigation errors of inertial navigation and encoder schemes will accumulate, and there will be a large error when used for a long time [2]. The visual scheme has high requirements for light and is sensitive to shadow, resulting in poor outdoor application effect.

At present, all inspection machines in substation field operation adopt the navigation and positioning mode of magnetic track guidance and RFID positioning, which requires embedding magnetic track on the running route of robot in advance and embedding RFID tags on the location where the robot needs to dock [3].

During the operation of the robot, the magnetic sensor array on the robot detects the deviation of the robot's motion center relative to the magnetic track and controls the difference between the left and right wheels through the motion controller, so that the robot can run along the set route. When the RFID card reader detects the label buried in the path, it notifies the robot to arrive at the set position. At this time, the robot can complete the detection of parking steering acceleration and deceleration equipment under the control of the car computer. Although this method has the characteristics of high repeatability of navigation and positioning and strong anti-interference ability, it also faces some problems in practice.For example, when magnetic track is laid, the ground construction is complicated and the workload is large, the robot running route is inflexible, and the height of the robot crossing the barrier is limited by the detection distance of the magnetic sensor, etc. These problems are difficult to solve under the existing methods [4].

2. Literature Review

In the current social development, electric power inspection robot is a kind of wheeled mobile robot. It can inspect outdoor high-voltage equipment in unattended or less attended substations by autonomous or remote control, collect operating status information of power equipment, timely find thermal defects, foreign body suspension, and other equipment anomalies of power equipment, and ensure the safety of power production. In terms of navigation mode, electric power inspection robot generally adopts magnetic track navigation. The magnetic sensor array installed in the front of the robot detects the deviation of the robot relative to the magnetic track and controls the robot to run along the magnetic track by means of two-wheel differential [5]. In practice, it is found that although the navigation method has centimeter-level navigation positioning accuracy, good repeatability, and strong anti-interference ability, the short detection distance of magnetic sensor results in the low chassis of the robot, and the obstacle crossing ability is not strong. In addition, the magnetic track navigation mode cannot feed back the precise position of the robot in the substation in real time, which is not conducive to the remote monitoring of the robot operation. At present, in addition to magnetic trajectory navigation, there are also inertial navigation, laser navigation, GPS navigation, and vision navigation for mobile robots. In view of the deficiency of magnetic trajectory navigation mode, considering that the inertial navigation positioning data are obtained by integral accumulation, the navigation accuracy will decrease with the passage of time, which is not suitable for long-term accurate positioning. At the same time, the outdoor environment has adverse effects on laser and visual navigation, while GPS navigation can directly learn the absolute position coordinates of the current measurement point from the GPS receiver, and its dynamic positioning accuracy can be up to centimeter level, and there is no error accumulation, so the coordinates of any position in the substation can be accurately obtained theoretically [6].

To solve the above problems, this paper proposes navigation and positioning technology analysis and research of electric inspection robot based on improved VMD- + ACO algorithm [7, 8].

3. Research Technique

3.1. Research on Improved VMD Algorithm

3.1.1. VMD Algorithm Research. VMD is a completely non-recursive decomposition algorithm; by constructing and solving the constrained variational problem, the signal is decomposed into K centre frequencies with $\{\omega\}$ center frequency. Compared with EMD algorithm, VMD algorithm has more strict mathematical model, overcomes the defects of EMD algorithm, can effectively separate intensive modes, and has been widely used in signal analysis, fault diagnosis, time series prediction, and other fields [9]. However, the selection of decomposition parameters of VMD, such as decomposition layers K and penalty factor α, has a great influence on the decomposition effect, and there is no clear theoretical guidance for its value.

The VMD computational complexity of the algorithm mainly depends on the iteration of the center frequency of each component and the equivalent FFT (fast Fourier transform) process, and the computational complexity of single FFT is O (NlgN). N refers to the length or sampling points of the analysis signal. Therefore, the computational complexity of decomposing a signal of length N into K components using VMD algorithm can be simply considered as the sum of the iterative consumption of the center frequency of all components and KO (NlgN) [10]. The computational complexity of EMD has been proved to be the same as FFT, both O (NlgN), which is an efficient decomposition algorithm. Therefore, VMD algorithm overcomes the inherent defects of EMD while sacrificing computational efficiency.

In addition, different from the adaptive decomposition of EMD, VMD is a completely non-recursive decomposition algorithm, whose decomposition effect is affected by the number of decomposition layers K and the value of penalty factor α [11]. If the number of decomposition layers is too much, the larger the penalty factor is, the narrower the bandwidth of the target signal will be, resulting in the redundant mode with multiple signal components belonging to the same main mode. On the contrary, if the bandwidth is too wide, the target signal will carry more noise and even contain other modal components. Too wide or too narrow bandwidth of the target signal will reduce the decomposition performance and affect the subsequent analysis results. At present, there is no clear theoretical basis for the value of decomposition parameters, which is very subjective and random.

3.1.2. Research on Improved VMD Algorithm. In order to solve the problem of VMD parameter selection, scholars at home and abroad constructed evaluation function based on envelope entropy orthogonal coefficient correlation coefficient and other parameters and used intelligent optimization algorithm to search the optimal value of decomposition layer K and penalty factor α simultaneously. Some achievements have been made in fault diagnosis and other fields. However, due to the limitation of the calculation efficiency of VMD algorithm, the optimization efficiency of large-scale hyperplane parameters is low, and the two-parameter or even multi-parameter optimization of VMD decomposition parameters will consume a lot of computing resources. The existing evaluation function of single index is not suitable for modal decomposition of vibration signals. Therefore, a new VMD optimization algorithm is proposed in this paper. The values of K and α are optimized separately, and the initialization process of the center frequency is optimized, so as to improve the efficiency of parameter optimization and give full play to the decomposition performance of VMD [12].

In the process of modal parameter identification, the accuracy of frequency identification is higher than that of damping, and even in most cases, the frequency range can be accurately estimated and the number of main modes can be judged according to the results of signal spectrum analysis

[13]. The goal of the VMD algorithm is to decompose the signal into K AM/FM signals with central frequency $\{\omega\ K\}$, which is essentially a narrowband filter bank with the center frequency of $\{\omega\ K\}$. Therefore, a simple peak method is used in this paper to determine the main modal number M and its corresponding central frequency {fi, $i = 1, 2, \ldots, M$} in advance. The decomposition parameter K is assigned as $K = M$, so the original multi-parameter optimization problem is simplified to the single-parameter optimization of penalty factor α, and the ADMM convergence process is accelerated to improve the calculation efficiency of VMD.

For the single-parameter optimization of penalty factor α, the evaluation function is established first, and the value of α is modified based on the posterior information of VMD decomposition results. However, because there is no clear functional relationship between α and the signal component finally decomposed, the analytic solution of the optimal value of α cannot be obtained directly by the established evaluation function. In addition, if traditional optimization methods (such as Newton method, simplex method, and so on) are adopted, the whole search space needs to be traversed, and VMD calculation efficiency is limited, so the search cannot be completed in a short time [14]. Therefore, intelligent optimization algorithms (such as genetic algorithm and particle swarm optimization algorithm) are also used in this paper to search for the optimal value of penalty factor α in the hyperplane.

The evaluation function established in this paper can accurately reflect the characteristic that each decomposed signal component contains only a single vibration mode and has no false component and redundant mode in the ideal state. The existing evaluation function of single index, such as envelop entropy orthogonal coefficient correlation, can represent the sparsity of signal. However, in the practical application process, negative optimization is easy to occur, which leads to the situation that the value of α is too large, and a group of harmonic signal components is decomposed [15]. This is due to the narrowband filtering characteristics of VMD. The larger the penalty factor α value is, the smaller the bandwidth of the signal component is, and finally the signal degenerates into a harmonic signal. Compared with the real target signal component, the harmonic signal component can get higher evaluation in the evaluation function of the above single index, resulting in the situation of negative optimization. However, this kind of harmonic signal is a false component, which only accounts for a very small part of the energy of the original signal. In order to facilitate the solution of the optimization algorithm, the following formula is used:

$$\text{fitness} = \left(1 - \sum_{k=1}^{K} \frac{u_k^2}{x^2}\right)\left(1 - \min\{\mathrm{r}(u_k, x)\}\right) \in (0, 1). \quad (1)$$

The essence of the optimization objective is to avoid false components or redundant modes, and the decomposed signal component has a large energy proportion and maintains a high correlation with the original signal [16]. Given the fitness function, the specific optimization algorithm adopted for solving the problem has little influence on the final optimization result, and the specific process of parameter optimization within the scope discussed in this paper is not shown in Figure 1.

3.2. Research on Improved ACO Algorithm

3.2.1. Basic ACO Principle and Mathematical Model Analysis. The ACO mathematical model is as follows: $G = (C, L)$ is a directed graph, $C = \{C1, C2, \ldots, C\}$ is a collection of N cities, $L = \text{lij|ci}$, cjCC is a collection of two connected cities, that is, two connected paths between cities, and dij (ij = 1, . . ., n) is the distance of lij.

Ant k ($k = 1, 2, \ldots, m$) is in the process of foraging; according to the probability selection formula, the following formula selects the next city.

$$\eta_{ij}(t) = \frac{1}{d_{ij}}. \quad (2)$$

The pheromone intensity Q represents the total amount of pheromones retained on the path after one cycle that affect ACO positive feedback function. ACO searches for the global optimal solution under the action of positive feedback. When Q is too large, the higher the total number of pheromones on the path is, the higher the probability that the searched path will be selected again, which will lead to the reduction of ant search range and global search ability, and ACO is prone to fall into the insufficient phenomenon of local optimal. If Q is too small, ants may enter into random path selection, which will cause ACO to fall into disordered disorder and ACO is prone to slow convergence [17].

To sum up, improper parameter setting and pheromone update lag are the reasons why basic ACO is prone to low convergence accuracy and slow convergence speed and fall into local optimal deficiency [18].

3.2.2. ACO Optimizing Design of Parameter. Improper setting of parameters such as pheromone heuristic factor α and expectation heuristic factor β leads to low convergence accuracy and slow convergence speed of basic ACO. The ACO parameter optimization design was carried out by combining the Python model and Matlab simulation calculation. Among them, TSP case base (ISPLIB) adopted Eil51 as the test library and designed variable expressions, as shown in the following formula:

$$X = [x_1, x_2, x_3, x_4, x_5],$$
$$E = \left\{ \begin{array}{l} x | x_j^i \le x_i \le x_j^j \\ i = 1, 2, 3, 4, 5, \\ j = 1, 2, 3, 4, 5 \end{array} \right\}. \quad (3)$$

The following parameters are optimized: the design variable of Nc and L, coefficient x_1 of the relationship between the number of ants and the number of cities, pheromone heuristic factor x_2, the expected heuristic factor x_3, pheromone volatilization coefficient x_4, pheromone intensity x_5. The curves of change relationship are shown in Figures 2–5, respectively.

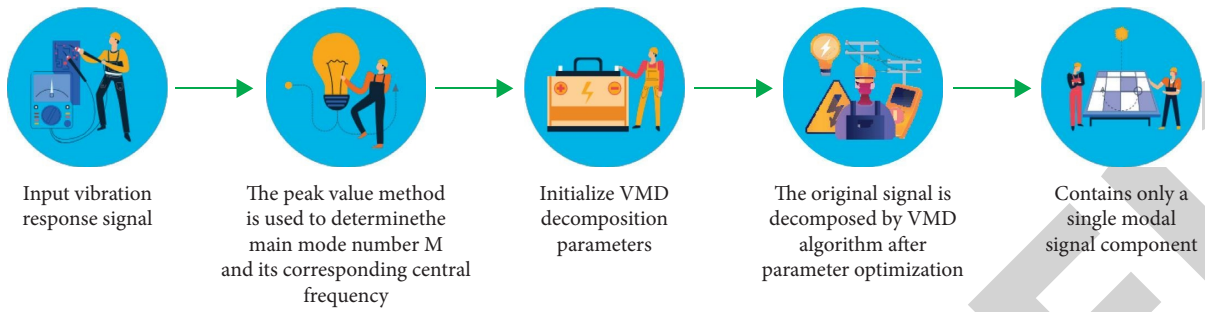

Figure 1: Flowchart of improved VMD algorithm.

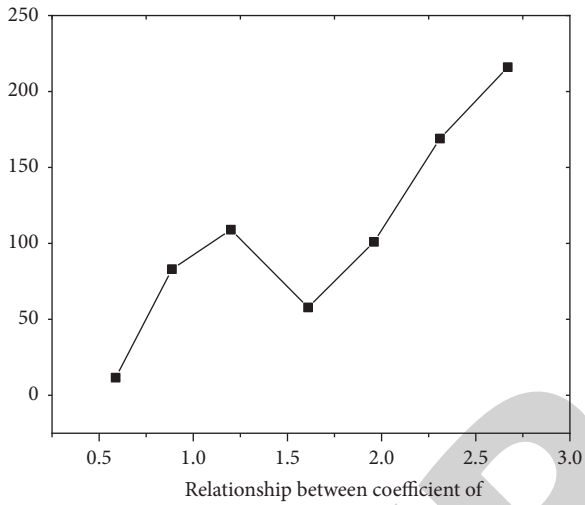

Figure 2: Variable ant quantity and city quantity relationship coefficient change curve.

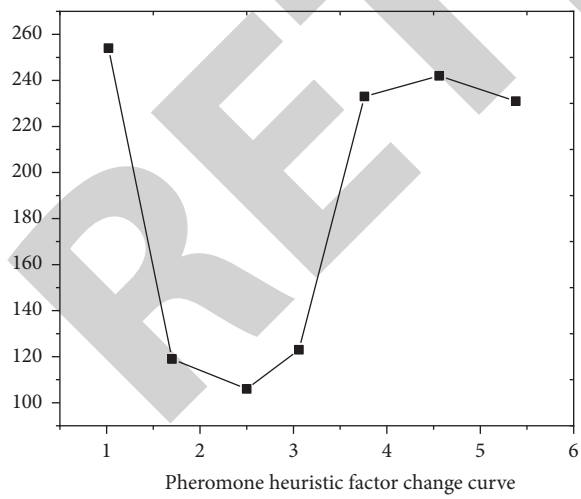

Figure 3: Graph of pheromone heuristic factor variation.

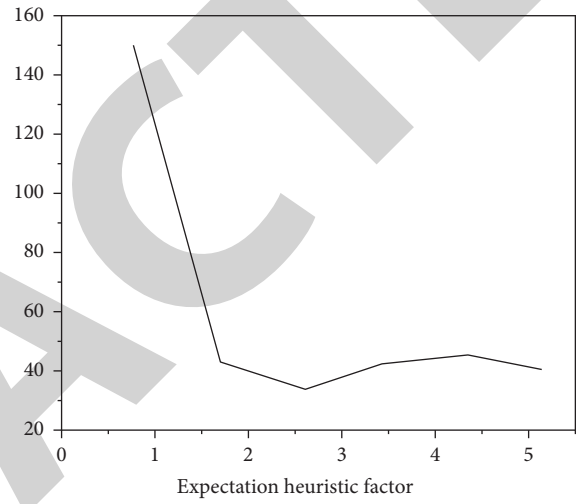

Figure 4: The expected heuristic factor change curve.

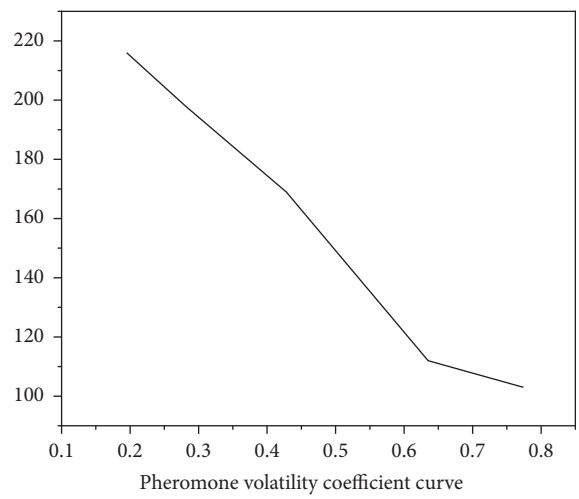

Figure 5: Pheromone volatilization coefficient curve.

Analysis shows that when x_1 (0.1 ~ 1.5) is set, N_C presents a downward quadratic function change trend with the increase of x_1, and L presents a decreasing trend. When x_1 (1.5 ~ 3.0), with the increase of x_1, N_C presents a first-order function increasing trend, and L is without significant change. Therefore, when x_1 is 1.5, N_C and L obtain the optimal values. When x_2 is (0.0 ~ 1.0), with the increase of x_2, N_C and L represent decreasing trend. When x_2 is (1.0 ~ 3.0), with the increase of x_2, N_C and L have no significant change. When x_2 is (3.0 ~ 6.0), N_C represents decreasing trend, and L represents increasing trend first and then has no significant change. Therefore, when [1.0 ~ 3.0]

Table 1: Maximum relative error and average relative error of the two methods.

Function	Algorithm	Optimal value	Worst-case value	Mean value	Minimum number of passes
F1 (x)	Basic ACO	0.15	0.96	0.58	148
	Improved ACO	0	0	0	112
F2 (x)	Basic ACO	0.07	0.59	0.26	139
	Improved ACO	0	0	0	101

is set, both N_C and L obtain the optimal value. When x_3 is (1.0 ~ 2.0), with the increase of x_3, N_C and L represent increasing trend. When x_3 is (2.04.0), with the increase of x_3, N_C and L have no significant change. When x_3 is (4.0 ~ 6.0), with the increase of x_3, N_C has no significant change, and L represents increasing trend. Therefore, when x_3 is $[2.0, 4.0]$, N_C and L obtain the best value. When x_4 is (0.0 ~ 0.9), with the increase of x_4, N_C and L represent decreasing trend. When x_4 is (0.5 ~ 0.7), with the increase of x_4, N_C and L approach two parallel lines. Therefore, when x_4 is $[0.5, 0.7]$, N_C and L obtain the best value. When x_5 is (10 ~ 1000), with the increase of x_5, N_C and L have no significant change. When x_5 is (10009000), with the increase of x_5, N_C represents decreasing trend, and L represents increasing trend. Therefore, when x_5 is $[10, 1000]$, N_C and L obtain the best value.

4. Interpretation of Result

In order to verify ACO performance, two multi-peak test functions with certain searching ability, Griewank function and Ackley function, were used to compare ACO and basic ACO, respectively, and the initial value range of variable dimension of the function was the theoretical optimal value [19].

The Griewank function and Ackley function of improved ACO and basic ACO were compared and analyzed for 10 performance test experiments, respectively, and the average value of 10 experiments was taken as the final result, as shown in Table 1 [20].

By analyzing the test results of Griewank function, the minimum iteration number of basic ACO is 148. The difference between the average value of 0.58 and the optimal value of 0.15 is 0.81 and 0.43, and the fluctuation errors are 540.00% and 286.67% compared with the optimal value. It shows that the convergence accuracy of basic ACO is not high. The minimum iteration number of improved ACO is 112, which is 24.32 less than that of basic. The mean value of the worst value and the optimal value of the function are both 0, indicating that the convergence accuracy of the improved ACO is higher and the number of iterations is significantly reduced [21, 22].

5. Conclusion

In order to meet the navigation and positioning requirements of force inspection robot, a new technology based on improved VMD- + ACO algorithm is proposed. The main content of this technology is based on the research of improved VMD algorithm and ACO algorithm, through the comparison of VMD algorithm and improved VMD algorithm. By using ACO parameter optimization design and so on, the research of improving VMD- + ACO algorithm navigation and positioning technology of electric inspection robot is finally established through experiments and analysis. The evaluation function established in this paper can accurately reflect the characteristic that each decomposed signal component contains only a single vibration mode and has no false component and redundant mode in the ideal state. Through experiments, the convergence accuracy of improved ACO is higher, and the number of iterations is significantly reduced. Based on the improved VMD- + ACO algorithm, it can meet the navigation and positioning requirements of electric inspection robot.

Data Availability

The data used to support the findings of this study are available from the corresponding author upon request.

Conflicts of Interest

The authors declare that they have no conflicts of interest.

References

[1] B. Ye and X. Song, "Research on an intelligent electric inspection robot," *Journal of Physics: Conference Series*, vol. 2005, no. 1, Article ID 012100, 2005.

[2] X. Yang, W. Zhao, and B. Song, "Thrust force calculation and analysis for the permanent magnet linear motor motion system considering the encoder errors," *IEEE Transactions on Industrial Electronics*, vol. 69, 2021.

[3] Y. Tao, L. Wu, J. Sidén, and G. Wang, "Monte Carlo-based indoor rfid positioning with dual-antenna joint rectification," *Electronics*, vol. 10, no. 13, p. 1548, 2021.

[4] N. Li, C. Zhang, S. Liu, C. Xie, and C. Li, "Design and study of intensive track laying system for single hole and double road in open cut station," *IOP Conference Series: Materials Science and Engineering*, vol. 780, no. 4, Article ID 042004, 2020.

[5] M. V. Petrenko, S. P. Dmitriev, A. S. Pazgalev, A. E. Ossadtchi, and A. K. Vershovskii, "Towards the non-zero field cesium magnetic sensor array for magnetoencephalography," *IEEE Sensors Journal*, vol. 21, 2021.

[6] J. Li, J. Lv, B. S. Oh, Z. Lin, and Y. J. Yu, "Identification of stress state for drivers under different gps navigation modes," *IEEE Access*, vol. 8, p. 1, 2020.

[7] Y. Chen and N. Shang, "Comparison of ga, aco algorithm, and pso algorithm for path optimization on free-form surfaces using coordinate measuring machines," *Engineering Research Express*, vol. 3, no. 4, Article ID 045039, 2021.

[8] J. Jia, C. Zhang, B. Yuan, Z. Chen, and J. Chen, "Development and process parameter optimization with an integrated test bench for rolling and forming strips of oolong tea," *Journal of Food Process Engineering*, vol. 44, no. 12, 2021.

[9] L. Zhang, C. Yu, and Y. Tan, "A method for pulse signal denoising based on vmd parameter optimization and grey

wolf optimizer," *Journal of Physics: Conference Series*, vol. 1920, no. 1, Article ID 012100, 2021.

[10] K. Chauhan, I. Mukhopadhyay, and D. B. Patel, "Fabrication of two component passive frequency filters by using cdte nanostructured thin films electrodeposited from ionic liquid medium," *ECS Meeting Abstracts*, vol. MA2020-02, no. 29, p. 1979, 2020.

[11] M. Brankovic, E. Gildin, R. L. Gibson, and M. E. Everett, "A machine learning-based seismic data compression and interpretation using a novel shifted-matrix decomposition algorithm," *Applied Sciences*, vol. 11, no. 11, p. 4874, 2021.

[12] J. Byun, A. Oddo, C. Porciani, and E. Sefusatti, "Towards cosmological constraints from the compressed modal bispectrum: a robust comparison of real-space bispectrum estimators," *Journal of Cosmology and Astroparticle Physics*, vol. 2021, no. 03, p. 105, 2021.

[13] R. Sihwail, O. S. Solaiman, K. Omar, K. Ariffin, and I. Hashim, "A hybrid approach for solving systems of nonlinear equations using harris hawks optimization and newton's method," *IEEE Access*, vol. 9, 2021.

[14] F. Xu, K. Yu, and L. Hua, "In-plane dynamic response and multi-objective optimization of negative Poisson's ratio (npr) honeycomb structures with sinusoidal curve," *Composite Structures*, vol. 269, no. 2, Article ID 114018, 2021.

[15] G. Reinert and C. Yang, "A bound on the rate of convergence in the central limit theorem for renewal processes under second moment conditions," *Journal of Applied Probability*, vol. 57, no. 1, pp. 343–360, 2020.

[16] R. Wang, K. Shi, and S. Wang, "Research on performance of artificial bee colony algorithm based on benchmark test function," *IOP Conference Series: Materials Science and Engineering*, vol. 740, no. 1, Article ID 012019, 2020.

[17] I. Negrin Diaz, E. Chagoyén Méndez, and A. Negrin Montecelo, "Parameter tuning in the process of optimization of reinforced concrete structures," *Dyna*, vol. 88, no. 216, pp. 87–95, 2021.

[18] M. Fan and A. Sharma, "Design and implementation of construction cost prediction model based on svm and lssvm in industries 4.0," *International Journal of Intelligent Computing and Cybernetics*, vol. 7, 2021.

[19] J. Jayakumar, S. Nagaraj, P. Chacko, and P. Ajay, "Conceptual implementation of artificial intelligent based E-mobility controller in smart city environment," *Wireless Communications and Mobile Computing*, vol. 2021, Article ID 5325116, 8 pages, 2021.

[20] J. Chen, J. Liu, X. Liu, X. Xu, and F. Zhong, "Decomposition of toluene with a combined plasma photolysis (cpp) reactor: influence of uv irradiation and byproduct analysis," *Plasma Chemistry and Plasma Processing*, vol. 41, 2020.

[21] R. Huang and X. Yang, "The application of TiO2 and noble metal nanomaterials in tele materials," *Journal of Ceramic Processing Research*, vol. 23, no. 2, pp. 213–220, 2022.

[22] Q. Zhang, "Relay vibration protection simulation experimental platform based on signal reconstruction of MATLAB software," *Nonlinear Engineering*, vol. 10, no. 1, pp. 461–468, 2021.